ELECTRONICS AND ELECTRICAL ENGINEERING
ISSN 1392 – 1215 *2011. No. 10(116)*
ELEKTRONIKA IR ELEKTROTECHNIKA

ELECTRICAL ENGINEERING
T 190
ELEKTROS INŽINERIJA

Penetration of Electric Field into Hollow Dielectric Bodies

M. Peric, S. Aleksic
University of Nis, Faculty of Electronic Engineering,
Nis, Serbia, phone: +381 18 529 423, e-mails: mika@elfak.rs, slavoljub.aleksic@elfak.ni.ac.rs

crossref http://dx.doi.org/10.5755/j01.eee.116.10.872

Introduction

Determination of electric field distribution inside dielectric bodies mostly requires solving the Laplace's equation. In many cases physical systems are so complex that analytical solutions are difficult or even impossible to obtain, as is mentioned in [1]. Nowadays, using computer, it is possible to exploit simple numerical approximation methods and in a few minutes to solve complex field problems.

A widely used method for numerical electrostatic problems solving is the Charge simulation method (CSM), described in [2]. Basic idea of this method is replacing the existing system by fictitious charges (FCs) chosen in certain way and placing them inside the respective system volumes. Unknown quantities are the charges values and their coordinates. The question remains how to form system of equations and to find these values? Several possibilities exist. One of the simplest options is to use the point matching method as shown in this paper. Other options exist, such as least – square method, variation method or boundary conditions method.

Using the point matching method a system of non – linear equations is formed in a way to satisfy boundary conditions for the system. Choice of initial values in iterative process of the solution, based on the linearization of the non – linear equations, can be difficult. In order to eliminate this problem it is convenient to use only the fictitious charges (FCs) as the unknowns. In [3, 4] authors suggest that FCs positions should be defined in advance. The electric field strength can be calculated from the system of linear equations using well known formulas for the electrostatic potential.

The problem of a dielectric hollow body placed in the homogeneous transverse steady electrostatic field, $\boldsymbol{E}_0 = E_0\hat{\boldsymbol{x}}$, as shown in Fig. 1, is considered in [5]. In this paper the CSM will be applied for the electric field calculation in an arbitrary shaped cavity of an arbitrary shaped dielectric body.

Theoretically, the precision of the solution depends on the number and positions of the FCs. Higher precision can be achieved by increasing the number of FCs.

The results of the electric field calculation based on the CSM are verified using the results from a commercial FEM program [6].

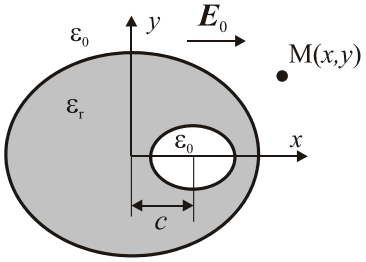

Fig. 1. Dielectric hollow body

CSM procedure

The dielectric system was divided into three respective FCs systems. The FCs were taken as the line or point charges placed at the cylindrical or spherical surfaces, depending on the problem geometry.

For determination of the potential outside the dielectric body, a total of N_1 FCs were placed inside the body (Fig. 2).

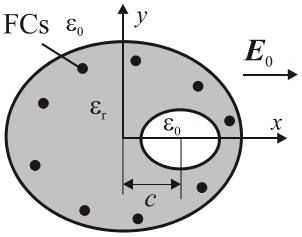

Fig. 2. Internal system of the FCs

For determination of the potential inside the dielectric body, a total of N_2 FCs were placed outside the body and a total of N_3 FCs inside the cavity (Fig. 3).

For determination of the potential inside the cavity, a total of N_4 FCs were placed inside the body, around the cavity (Fig. 4).

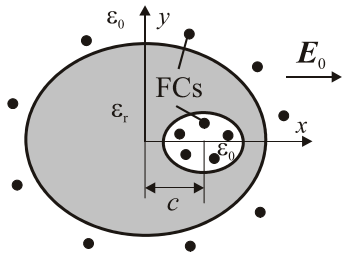

Fig. 3. External system of the FCs

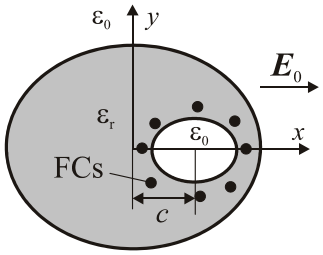

Fig. 4. The system of FCs for determination of the potential inside the cavity

The electrical potential is given by

$$\varphi(x,y)=\sum_j p_j(x,y)q_j\,, \tag{1}$$

where q_j represents the (unknown) magnitude of the j^{th} charge and $p_j(x,y)$ is the coefficient that depends only on the type of the distribution and position of the observation point $\mathrm{M}(x,y)$. The intensities of the FCs can be determined after solving the system of linear equations satisfying the boundary conditions on the system surface and on the surface which separates the layers (the dielectric layers and the cavity).

In order to demonstrate the application of the CSM procedure, several examples are presented.

Dielectric circular cylinder with an eccentric circular cavity

A dielectric circular cylinder with an eccentric circular cavity placed in a transverse electrostatic field, is analysed in [7]. The cylinder has radius a, eccentricity c, and radius of the cavity b (Fig. 5).

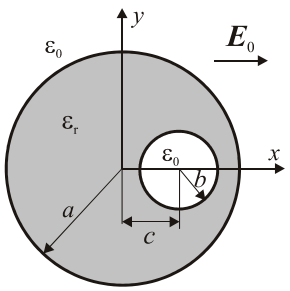

Fig. 5. Dielectric cylinder with circular cavity

Applying the CSM, the whole system was divided into three systems with FCs, according to the procedure described in the previous section. The FCs are line charges placed at the cylindrical surfaces with circular cross-section. The radius of the cylindrical surfaces was determined by coefficients f_i $(i=1,2,3,4)$. N_1 fictitious charges were placed inside the body's volume, at points $x_{1j}=f_1 a\cos\theta_{1j}$ and $y_{1j}=f_1 a\sin\theta_{1j}$, $0<f_1<1$

$$\theta_{1j}=\pi\frac{2j-1}{N_1},\ j=1,...,N_1\,. \tag{2}$$

The electric potential outside the dielectric cylinder can be expressed as

$$\varphi_{\mathrm{I}}=\varphi_0-\sum_{j=1}^{N_1}\frac{q'_{1j}}{2\pi\varepsilon_0}\ln\sqrt{(x-x_{1j})^2+(y-y_{1j})^2}\,, \tag{3}$$

where q'_{1j} $(j=1,...,N_1)$ are the unknown line charges placed at the cylindrical surface. The coordinates $(x_{1j},\ y_{1j})$ are their positions and the constant $\varphi_0=-E_0x$.

For determination of the potential inside the dielectric body and inside the cavity, the second system was formed. The potential inside this system was

$$\varphi_{\mathrm{II}}=-\sum_{\mathrm{j}=1}^{N_2}\frac{q'_{2\mathrm{j}}}{2\pi\varepsilon}\ln\sqrt{(x-x_{2j})^2+(y-y_{2j})^2}\ -$$
$$-\sum_{\mathrm{k}=1}^{N_3}\frac{q'_{3\mathrm{k}}}{2\pi\varepsilon}\ln\sqrt{(x-x_{3k})^2+(y-y_{3k})^2}\,, \tag{4}$$

where q'_{2j} $(j=1,...,N_2)$ and q'_{3k} $(k=1,...,N_3)$ are unknown line charges placed at the cylindrical surfaces and $(x_{2j},\ y_{2j})$ and $(x_{3k},\ y_{3k})$ are their positions $x_{2j}=f_2 a\cos\theta_{2j}$, $y_{2j}=f_2 a\sin\theta_{2j}$, $f_2>1$

$$\theta_{2j}=\pi\frac{2j-1}{N_2},\ \text{for}\ j=1,...,N_2 \tag{5}$$

and $x_{3k}=c+f_3 b\cos\theta_{3k}$, $y_{3k}=f_3 b\sin\theta_{3k}$, $0<f_3<1$

$$\theta_{3k}=\pi\frac{2k-1}{N_3},\ \text{for}\ k=1,...,N_3\,. \tag{6}$$

For third system, the electrical potential inside the cavity was

$$\varphi_{\mathrm{III}}=-\sum_{j=1}^{N_4}\frac{q'_{4j}}{2\pi\varepsilon_0}\ln\sqrt{(x-x_{4j})^2+(y-y_{4j})^2}\,, \tag{7}$$

where q'_{4j} $(j=1,...,N_4)$ are unknown line charges placed at the cylindrical surface and $(x_{4j},\ y_{4j})$ are their coordinates $x_{4j}=c+f_4 b\cos\theta_{4j}$, $y_{4j}=f_4 b\sin\theta_{4j}$, $f_4>1$

$$\theta_{4j}=\pi\frac{2j-1}{N_4},\ \text{for}\ j=1,...,N_4\,. \tag{8}$$

A system of the linear equations was formed using

the point matching method in a way to satisfy boundary conditions for the electrical potential and the normal component of the electric field at the system boundaries.

The total number of unknowns was $N = N_1 + N_2 + N_3 + N_4$ (N_i ($i = 1,2,3,4$) was the total number of the fictive charges per unit length in each system). After solving this system, the unknown values of the FCs were determined and the electric field could be calculated.

The electrostatic field vector components outside the body are:

$$E_{1x} = E_0 + \sum_{j=1}^{N_1} \frac{q'_{1j}}{2\pi\varepsilon_0} \frac{(x - x_{1j})}{(x - x_{1j})^2 + (y - y_{1j})^2}, \quad (9)$$

$$E_{1y} = \sum_{j=1}^{N_1} \frac{q'_{1j}}{2\pi\varepsilon_0} \frac{(y - y_{1j})}{(x - x_{1j})^2 + (y - y_{1j})^2}. \quad (10)$$

Inside the body the electrostatic field vector components are:

$$E_{2x} = \sum_{j=1}^{N_2} \frac{q'_{2j}}{2\pi\varepsilon} \frac{(x - x_{2j})}{(x - x_{2j})^2 + (y - y_{2j})^2} + \sum_{k=1}^{N_3} \frac{q'_{3k}}{2\pi\varepsilon} \frac{(x - x_{3k})}{(x - x_{3k})^2 + (y - y_{3k})^2}, \quad (11)$$

$$E_{2y} = \sum_{j=1}^{N_2} \frac{q'_{2j}}{2\pi\varepsilon} \frac{(y - y_{2j})}{(x - x_{2j})^2 + (y - y_{2j})^2} + \sum_{k=1}^{N_3} \frac{q'_{3k}}{2\pi\varepsilon} \frac{(y - y_{3k})}{(x - x_{3k})^2 + (y - y_{3k})^2}. \quad (12)$$

The electrostatic field vector components inside the cavity are:

$$E_{3x} = \sum_{j=1}^{N_4} \frac{q'_{4j}}{2\pi\varepsilon_0} \frac{(x - x_{4j})}{(x - x_{4j})^2 + (y - y_{4j})^2}, \quad (13)$$

$$E_{3y} = \sum_{j=1}^{N_4} \frac{q'_{4j}}{2\pi\varepsilon_0} \frac{(y - y_{4j})}{(x - x_{4j})^2 + (y - y_{4j})^2}. \quad (14)$$

Results for dielectric circular cylinder with an eccentric circular cavity

A convergence of the electric field results for a different number of FCs is shown in Table 1, where $N_e = N_1 = N_2 = N_3 = N_4$.

The results are given for the two characteristic observation points: the centre of the body with coordinates $(0, 0)$ and the centre of the cavity with normalized coordinates $(0.45, 0)$. The input data are: $f_1 = 0.9$, $f_2 = 1.2$, $f_3 = 0.9$, $f_4 = 1.1$, $b/a = 0.25$, $c/a = 0.45$, $\varepsilon_r = 3$. As the number of FCs increases, convergence of the results becomes better. But, for $N_e > 150$, the system of the linear equations becomes irregular because the FCs come very close to each other and a problem of division by zero appears. When $N_e = 120$, the results converge at 4 to 5 decimal places.

The electric field components, E_x and E_y, along the x-axis in the cavity, are presented in Fig. 6. From Fig. 6 it can be seen that the electric field vector is homogeneous in the cavity. The E_x component is almost constant, while the value of the E_y component is negligible.

Table 1. Normalized electrostatic field strength, E/E_0, at the observation point $M(x/a, y/a)$ for a different number of the FCs

N_e	M(0, 0)	M(0.45, 0)
5	0.296062	0.219725
10	0.406967	0.458361
30	0.438597	0.732438
50	0.430652	0.764120
80	0.429240	0.768651
100	0.429184	0.768871
120	0.429177	0.768904

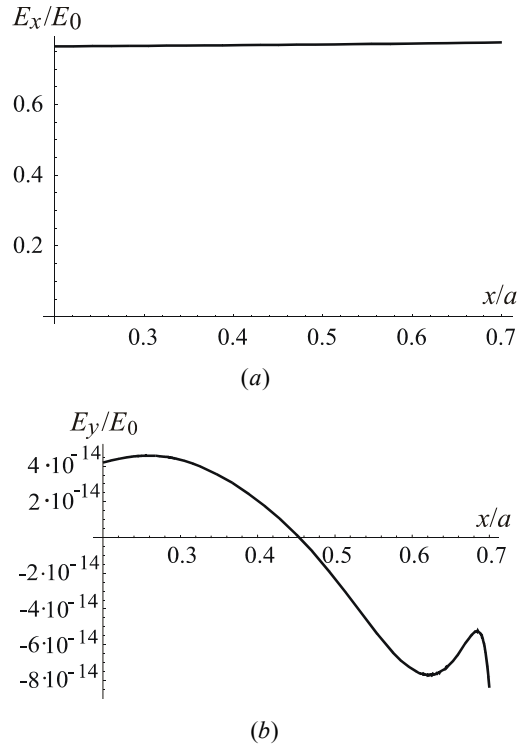

Fig. 6. Distribution of E_x (a) and E_y (b) electric field components along x-axis in cavity

Fig. 7 – Fig. 10 show how the boundary conditions were satisfied for the tangential components of the electric field vector at the separation surfaces air - dielectric and dielectric – cavity.

In the ideal case these components should be equal. Fig. 7 – Fig. 10 are given for the different values of the coefficients f_i ($i = 1,2,3,4$) and the different number of the FCs. A good satisfaction of the boundary conditions was achieved with an increased number of the FCs. However, better satisfaction of the boundary conditions was obtained when the FCs were a little further from the

separating surfaces (Fig. 8 and Fig. 10). In that case the obtained accuracy was 10^{-6}-10^{-9}.

In Table 2, the CSM results for the electric field at the observation point M(0.4,0.0) are compared to the results obtained from a commercial FEM program [6] and COMSOL [8]. The external electric field was taken to be $E_0 = 100\,\mathrm{V/m}$. The results were found to be in a very good agreement (relative error was less than 2%).

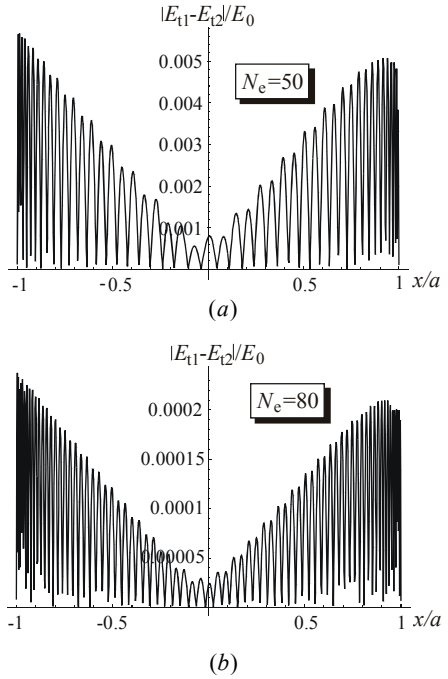

Fig. 7. Deviation of the tangential electric field component at the air-dielectric boundary for $f_1 = 0.9$, $f_2 = 1.2$, $f_3 = 0.9$, $f_4 = 1.1$ and a different number of FCs

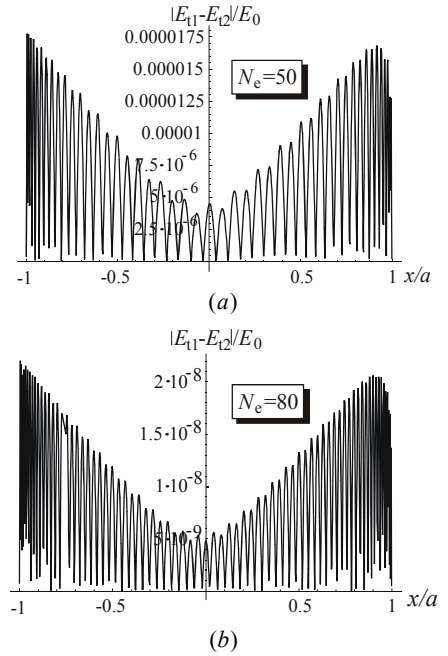

Fig. 8. Deviation of the tangential electric field component at the air-dielectric boundary for $f_1 = 0.8$, $f_2 = 1.4$, $f_3 = 0.6$, $f_4 = 1.2$ and a different number of FCs

Table 2. Results of comparison

Applied method	E / E_0
CSM	0.76785
Finite element method (femm 4.2)	0.77945
Finite element method (COMSOL)	0.77959

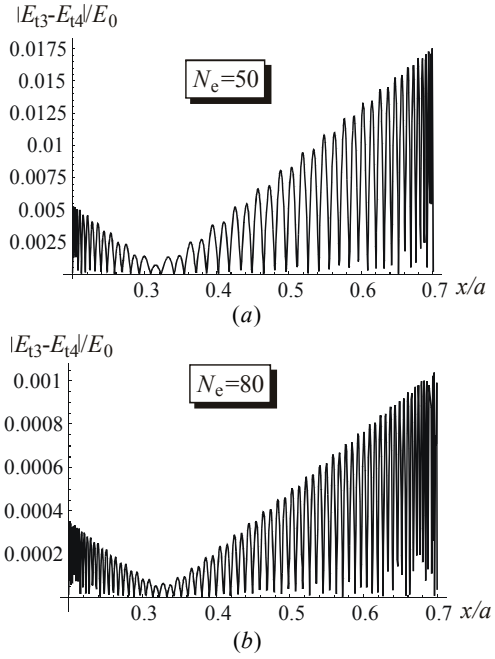

Fig. 9. Deviation of the tangential electric field component at the dielectric-cavity boundary for $f_1 = 0.9$, $f_2 = 1.2$, $f_3 = 0.9$, $f_4 = 1.1$ and a different number of FCs

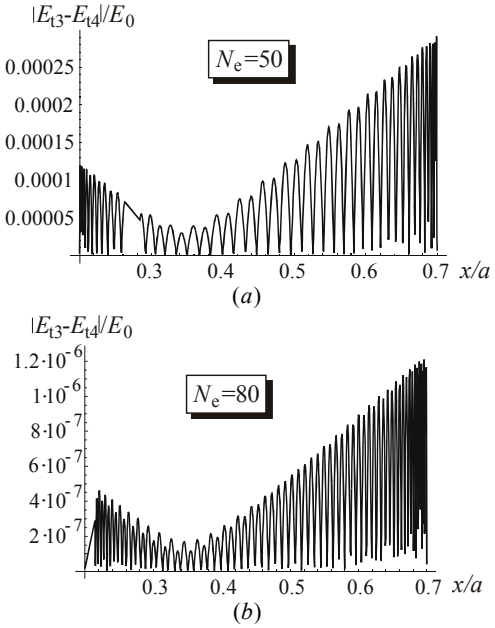

Fig. 10. Deviation of the tangential electric field component at the dielectric-cavity boundary for $f_1 = 0.8$, $f_2 = 1.4$, $f_3 = 0.6$, $f_4 = 1.2$ and a different number of FCs

Determination of FCs optimal positions

It was evident that the positions of the FCs had a great influence on the CSM results. If the FCs were very

close or too far from the cylindrical surfaces the obtained error was higher. Lately a large number of optimisation methods have been developed, such as genetic algorithm, presented in [9]. In this paper, optimal positions of the FCs were determined for one simple example. An analytical solutions for the problem of a cavity in a dielectric medium in a homogeneous transverse electrostatic field, Fig. 11, obtained after solving Laplace's equation, is given in [10]. The expression for the electric field inside the cavity is

$$E = \frac{2\varepsilon_r}{\varepsilon_r + 1} E_0 \geq E_0 . \quad (15)$$

For $\varepsilon_r = 3$ normalized electrostatic field strength is $E / E_0 = 1.5$. Applying the CSM, the FCs will be the line charges placed at the cylindrical surfaces around the circular cross-section.

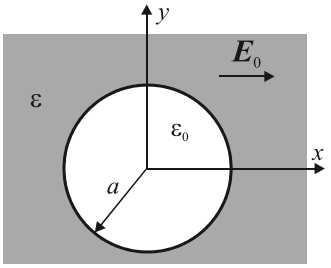

Fig. 11. Cylindrical cavity in a homogeneous dielectric medium

Cylindrical surfaces radii were defined by the coefficients f_i $(i = 1, 2)$. Boundary conditions for the potential and the electric field should be satisfied at the boundary surfaces as previously described. In that way a system of linear equations was formed. Solving this system, the potential and the electric field strength could be determined. Optimal positions of the FCs can be determined varying the positions of the FCs. The best results were determined by comparison with the analytical results. The electric field values for the different number of the FCs are shown in Table 3. The coefficients f_i are known: $f_1 = 0.7$ and $f_2 = 1.2$. The results gave good convergence, but, the chosen values of the coefficients f_i did not give an exact solution obtained by analytical method, $E / E_0 = 1.5$.

Table 3. Normalized electric field strength, E / E_0, inside the cavity for $\varepsilon_r = 3$ and a different number of the FCs

N	E / E_0
5	0.90212907938
10	1.27983669740
30	1.49572751017
50	1.49989337464
100	1.49999998862

So, a procedure for the FCs optimal position determination was reapplied. Using this procedure, the number of the FCs was known, but the coefficients f_i changed their values between $0.1 < f_1 < 0.9$ and $1.1 < f_2 < 1.5$, with a step 0.1. For every value of the coefficients f_i the electric field has been calculated and compared with the analytical value. In Table 4 the optimal values of the coefficients f_i are shown, when the number of the FCs was $N = 70$. The discrete electric field values inside the cavity for the different values of coefficients f_1 and f_2 and the different number of FCs, N, are shown in Fig. 12 and Fig. 13.

Table 4. FCs optimal positions, for $\varepsilon_r = 3$ and $N = 70$

f_1	f_2	E / E_0
0.10	1.5	1.50000000000
0.20	1.5	1.50000000000
0.30	1.5	1.50000000000
0.40	1.5	1.50000000000
0.50	1.5	1.50000000000
0.60	1.5	1.50000000000

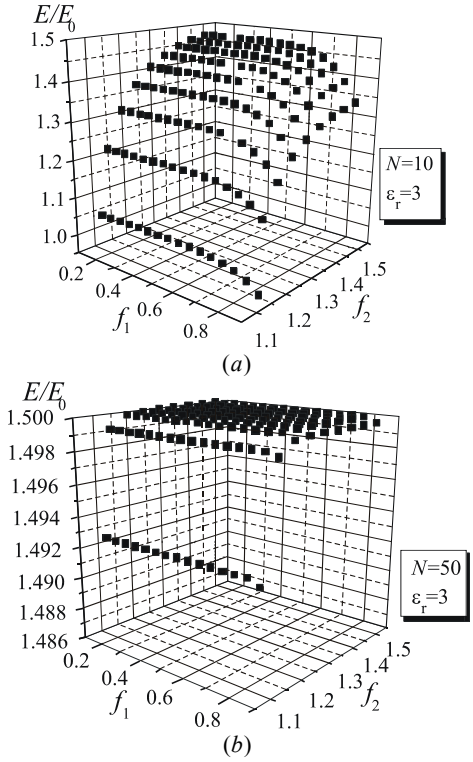

Fig. 12. Normalized electric field discrete values inside the cavity

In Fig. 12, a 3D presentation of the electric field for the different FCs number is shown. For better view the obtained solutions are presented in the $E - f_2$ plane in Fig. 13. It can be seen that for an increased number of the FCs, the electric field values are grouping around the analytical value. In Table 5 the results obtained using CSM have been compared with the FEMM and COMSOL results as well as with the analytical solution. A very good agreement was found (an error less than 1.6%).

An application of the CSM for calculation of the electrostatic field inside an arbitrary shaped hollow dielectric body is presented. The body was placed in the homogeneous transverse electrostatic field. Described procedure can be applied for calculation of the penetrated electric field in some human tissues in living and working environments. The correct choice of the FCs was found

very important. The most commonly used FCs, depending on the problem geometry, are point, line and ring charges.

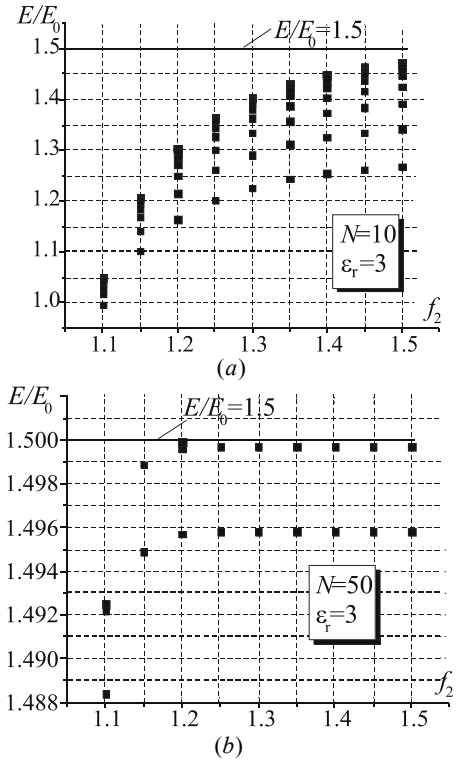

Fig. 13. Normalized electric field discrete values inside the cavity

Table 5. Results of the comparison

Applied method	E / E_0
Analytical solution	1.50000
CSM ($N = 100$, $f_1 = 0.7$, $f_2 = 1.3$)	1.50000
Finite element method (femm 4.2)	1.47522
Finite element method (COMSOL)	1.47679

The most important questions were: How to place the FCs, which is their optimal number and how to choose the matching points? The answers on these questions depend on the experience of the investigators.

Conclusions

The obtained results showed that the precision of the solution depends on the number of the FCs. Higher precision can be achieved by increasing the number of the FCs. The number of the FCs can't be too large because the system of the equations could be ill conditioned. In the examples presented here, a good convergence was obtained for N=(50÷80) FCs per system. A good satisfaction of the boundary conditions was accomplished with an increased number of the FCs. Also, better results were obtained when the FCs were a little further from the boundaries. In that case the obtained accuracy was 10^{-6} -10^{-9}. The obtained CSM results have been compared with the FEMM and COMSOL results. The results were in a good agreement, because the error was less than 2%.

References

1. **Brauer H.** Computation of electromagnetic fields using integral methods // Intern. PhD Seminar – Computation of Electromagnetic Field. – Montenegro, 2004. – P. 201–212.
2. **Singer H., Steinbigler H., Weiss P.** A charge simulation method for the calculation of high voltage fields // IEEE Trans. – PAS–73, 1974. – P. 1660–1668.
3. **Surutka J. V., Velickovic D. M.** Some improvements of the Charge Simulation Method for Computing Electrostatic Fields. // Bulletin LXXIV de l'Academie Serbe des Sci. et des Arts, 1981. – No. 15. – P. 27–44.
4. **Velickovic D. M., Dincov D.** One New Approach to Calculation of Multiwire Lines. // 3rd International Conference TELSIKS 97. – Nis, YU, 1997. – P. 604–607.
5. **Peric M. T.** Penetration of electric field into hollow bodies, Master thesis. – Nis, 2006.
6. **Femm 4.2.** Online: http://www.femm.info.
7. **Peric M.** Dielectric Body with Arbitrary Shaped and Positioned Cavity in Homogeneous Transversal Electric Field // Serbian Journal of Electrical Engineering. Serbia and Montenegro, 2004. – Vol. 1. – No. 2. – P. 175–186.
8. **COMSOL Multiphysics.** Online: http://comsol.com.
9. **Nishimura R., Nishimori K., Ishihara N.** Determining the arrangement of fictitious charges in charge simulation method using genetic algorithms // Journal of Electrostatics, 2000. – Vol. 49. – Iss. 1–2. – P. 95–105.
10. **Peric M., Aleksic S.** Fictitious charges arrangement determination in Charge Simulation Method // 51st Intern. Wissenschaftliches Kolloquium. – TU Ilmenau, Germany, 2006.

Received 2010 10 12
Accepted after revision 2011 02 14

M. Peric, S. Aleksic. Penetration of Electric Field into Hollow Dielectric Bodies // Electronics and Electrical Engineering. – Kaunas: Technologija, 2011. – No. 10(116). – P. 19–24.

Electrostatic field distribution inside dielectric hollow bodies of different shapes was determined using Charge Simulation Method. The obtained results were compared with a commercial software results. Determination of the optimal positions of fictitious charges in the Charge Simulation Method was also considered. The results are presented graphically and in tables. Ill. 13, bibl. 10, tabl. 5 (in English; abstracts in English and Lithuanian).

M. Peric, S. Aleksic. Elektrinio lauko įsiskverbimas į tuščiavidurius dielektrinius kūnus // Elektronika ir elektrotechnika. – Kaunas: Technologija, 2011. – Nr. 10(116). – P. 19–24.

Elektrinio lauko pasiskirstymas tuščiaviduriuose dielektriniuose kūnuose buvo nustatytas taikant krūvio imitavimo metodą. Gauti rezultatai palyginti su komercinės programos rezultatais. Aptarta, kaip, taikant krūvių imitavimo metodą, nustatomos optimalių fiktyvių krūvių vietos. Rezultatai pateikti grafiškai ir lentelėse. Il. 13, bibl. 10, lent. 5 (anglų kalba; santraukos anglų ir lietuvių k.).